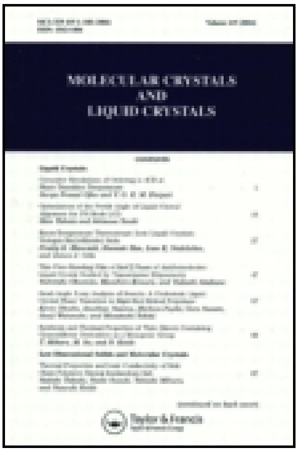

Molecular Crystals and Liquid Crystals
Publication details, including instructions for authors and subscription information:
http://www.tandfonline.com/loi/gmcl20

Synthesis and Characterization of Ferroelectric Liquid Crystalline Siloxanes Containing 4-Hydroxyphenyl(2S,3S)-2-Chloro-3-Methylvalerate

Chih-Hung Lin [a]

[a] Center for General Education, Chang Gung University of Science and Technology, Kwei-Shan, Tao-Yuan, Taiwan, Republic of China

To cite this article: Chih-Hung Lin (2012): Synthesis and Characterization of Ferroelectric Liquid Crystalline Siloxanes Containing 4-Hydroxyphenyl(2S,3S)-2-Chloro-3-Methylvalerate, Molecular Crystals and Liquid Crystals, 552:1, 33-42

To link to this article: http://dx.doi.org/10.1080/15421406.2011.599204

Mol. Cryst. Liq. Cryst., Vol. 552: pp. 33–42, 2012
Copyright © Taylor & Francis Group, LLC
ISSN: 1542-1406 print/1563-5287 online
DOI: 10.1080/15421406.2011.599204

Synthesis and Characterization of Ferroelectric Liquid Crystalline Siloxanes Containing 4-Hydroxyphenyl(2S,3S)-2-Chloro-3-Methylvalerate

CHIH-HUNG LIN*

Center for General Education, Chang Gung University of Science and Technology, Kwei-Shan, Tao-Yuan, Taiwan, Republic of China

New series of organosiloxane ferroelectric liquid crystalline materials have been synthesized, and their mesomorphic and physical properties have been characterized. These new series contain bis-siloxane or tris-siloxane unit attached to the flexible alkyl chain end of (2S,3S)-2-chloro-3-methylvalerate. The siloxane molecule induction is helpful to the chiral smectic C (S_C) formation and chiral S_C* stabilization, and it simultaneously causes the liquid crystal temperature range of chiral S_C* to be broader. The siloxane member is helpful in reducing the smectic C (S_C) transation shift temperature, and the molecule containing tris-siloxane units shows better effect than the bis-siloxane one. The synthesis and characterization of the new FLCs materials which exhibit S_C* phase at room temperature and higher spontaneous polarization are presented.*

Keywords Ferroelectric liquid crystal; siloxane; spontaneous polarization

Introduction

With the development of optoelectronics, the transposition of ferroelectricity to anisotropic liquids and, in particular, to thermotropic liquid crystals, found in Rochelle salts (potassium and sodium tartrate) [1] at the beginning of the 20th century, has been a matter of great interest for the past two decades [1,3]. The molecular design of these compounds was directly deduced from the original work of Mayer and Coles who predicted, using a symmetry argument, that tilted smectic phases obtained with chiral molecules have a transverse dipole moment and should exhibit an electric spontaneous polarization [4,5].

Ferroelectric liquid crystal (FLC) materials exhibiting SmC* phase at room temperature and low melting temperatures are of great interest to researchers in the electro-optic field [6–11]. These are the basis of a variety of potential devices ranging from large-area flat-panel displays, ultrafast electro-optic modulators, and spatial light modulators [12–16]. S_C* materials are suited for gray-scale applications.

FLC molecules consist of a rigid core and end-tail groups with a chiral center located on one or both groups. For most FLC molecules, the end-tail groups are hydrocarbon chains. When varying the hydrocarbon chain lengths of the molecules, the macroscopic properties are modified. For example, the rotational viscosity as well as the tilt angle of

---

Address correspondence to Chih-Hung Lin, Center for General Education, Chang Gung University of Science and Technology, 261, Wen-Hwa 1st Road, Kwei-Shan, Tao-Yuan, Taiwan, Republic of China. E-mail: chlin@gw.cgit.edu.tw the S_C molecules increase with increasing chain length. The case of the variation of the spontaneous polarization, *Ps*, as a function of chain length is less obvious. To crystallize FLC molecule easily, increasing the length of the nonpolar moiety helps to dilute the transverse dipole moment in the molecule which thus decrease the value of *Ps*, whereas the increase of the tilt angle should have a tendency to increase *Ps*.

In this study, we designed and prepared a new series of molecule, which contains a two-chiral center and the partial substitution of hydrocarbon chains by more flexible dimethylsiloxyl and trimethylsiloxyl groups. Thus it was expected to enhance the thermal stability and *Ps* value of the FLC material [17–19].

Experimental

^{1}H-NMR spectra were recorded on a Varian VXR-300 or Bruker 300 MHz spectrometer. Thermal transitions and thermodynamic parameters were determined using a Seiko SSC/5200 differential scanning calorimeter (DSC) equipped with a liquid nitrogen cooling accessory. Heating and cooling rates were 10°C/min. Thermal transition reports were collected during the second heating and cooling scans. A Nikon Microphot-FX polarized optical microscope (POM) equipped with a Mettler FP 82 hot stage and a FP 80 central processor was used to observe the thermal transitions and to analyze the anisotropic textures. Polymerization reactions were traced using a Nicolet 520 FT-IR spectrometer.

Synthesis

The general synthetic routes of the intermediates and target molecule are shown in Scheme 1. The purity and chemical structures of the intermediates and target compounds can be easily verified by TLC and ^{1}H-NMR spectroscopy. The synthetic procedures and chemical analyses of each product are described sequentially below.

Compounds (1)–(5)

4-(2-Propenyloxy)biphenyl-4′-ol (1)
4-(5-Hexenyloxy)biphenyl-4′-ol (2)
4-(8-Nonenyloxy)biphenyl-4′-ol (3)
4-(9-Decenyloxy)biphenyl-4′-ol (4)
4-(10-Undecenyloxy)biphenyl-4′-ol (5)

Compounds (1)–(5) were prepared by the same method. The synthesis of compound (1) is described below.

4,4′-Dihydroxydiphenyl (7.9 g, 0.0425 mol) was added to a solution of potassium hydroxide (4.76 g, 0.085 mol) in ethanol (300 mL, 95%). Potassium iodide (0.2 g) was also added and the solution was heated to reflux for 0.5 h. 3-Bromopropene (3.0 g, 0.025 mol) was then slowly added and the solution was refluxed overnight. The solution was cooled and poured into 50 mL of 6N HCl, and the solid salt was removed by filtration. The remaining white solid was recrystallized from ethanol to yield 2.43 g (43%) of white crystals [mp = 140.5°C. ^{1}H-NMR ($CDCl_3$, δ, ppm): 4.50–4.70 (t, 2H, $-O-C\underline{H}_2-CH=$), 5.00 (s, 1H, $\underline{H}O-$), 5.31 (m, 2H, $=C\underline{H}_2$), 6.08 (m, 1H, $CH_2-C\underline{H}=$), 6.80–7.60 (m, 8H, aromatic protons)].

Compound (6)

(2S,3S)-2-Chloro-3-methylvaleric acid (6)

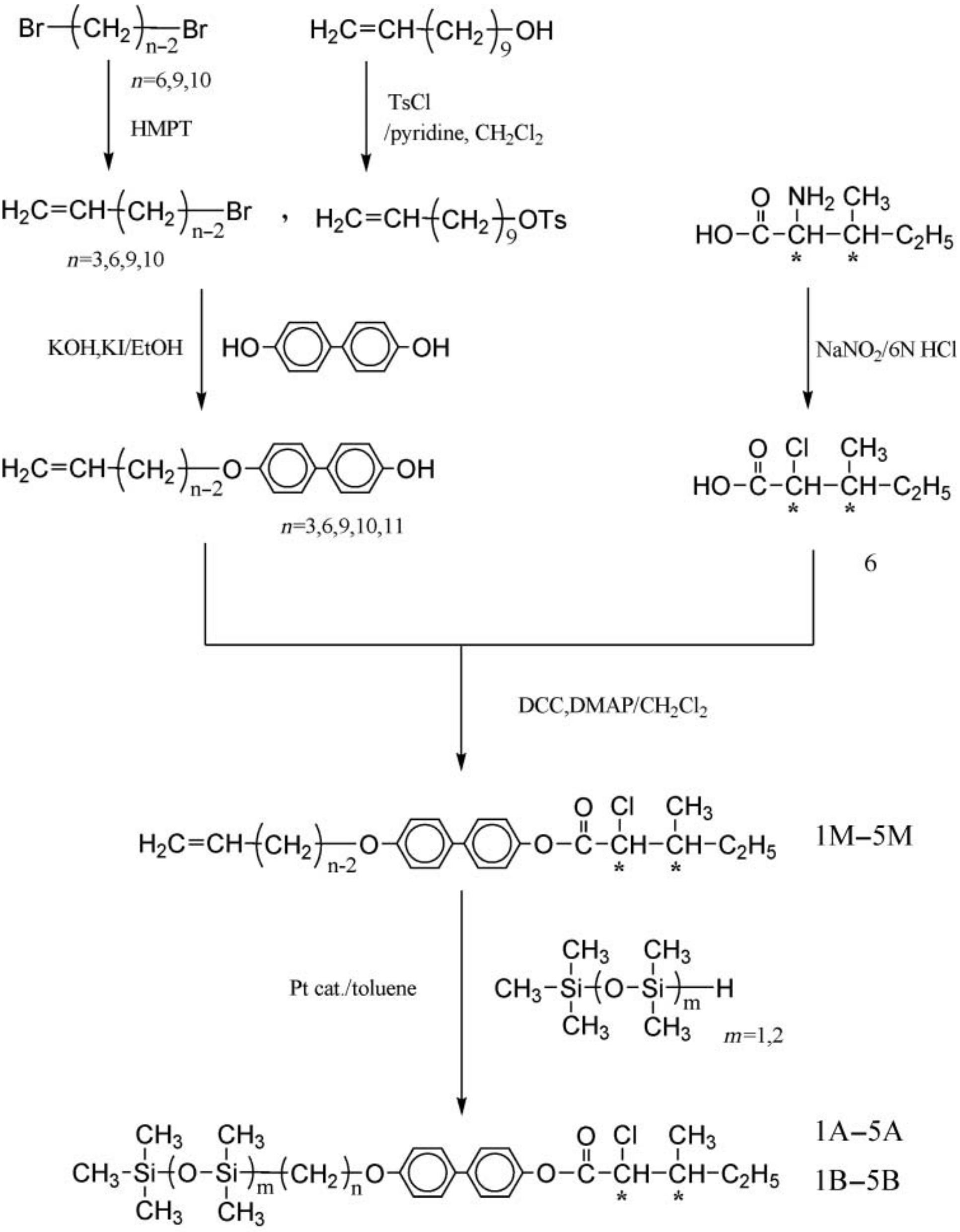

	1A	2A	3A	4A	5A	1B	2B	3B	4B	5B
m	1	1	1	1	1	2	2	2	2	2
n	3	6	9	10	11	3	6	9	10	11

Scheme 1. Synthesis of compounds (1M)–(5M), (1A)–(5A), and (1B)–(5B).

L-Isoleucine (9.7 g, 0.074 mol) was dissolved in 250 mL of 6N HCl and slowly added to sodium nitrite powder (10.2 g, 0.148 mol). This solution was allowed to stand at 0°C–5°C for 20 h by ice bath. The solution was then extracted by 200 mL of dichloromethane. The extraction solution was washed with saturated sodium chloride (aq.) and dried over anhydrous magnesium sulfate. After removal of the solvent by evaporation under reduced pressure, the residue was purified by distillation under reduced pressure to yield 5.79 g (52%) of colorless liquids [^{1}H-NMR (CDCl$_3$, δ, ppm): 0.78–1.04 (m, 6H, $-\mathrm{C\underline{H}_3}$), 1.20–2.10 (m, 3H, $-\mathrm{C\underline{H}-C\underline{H}_2-CH_3}$), 4.16 (d, 1H, $-\mathrm{C\underline{H}Cl-COOH}$), 9.95 (s, 1H, $-\mathrm{COO\underline{H}}$)].

Compounds (1M)–(5M)

4-(2-Propenyloxy)biphenyl-4′-yl(2S,3S)-2-chloro-3-methylvalerate (1M)
4-(5-Hexenyloxy)biphenyl-4′-yl(2S,3S)-2-chloro-3-methylvalerate (2M)
4-(8-Nonenyloxy)biphenyl-4′-yl(2S,3S)-2-chloro-3-methylvalerate (3M)
4-(9-Decenyloxy)biphenyl-4′-yl(2S,3S)-2-chloro-3-methylvalerate (4M)
4-(10-Undecenyloxy)biphenyl-4′-yl(2S,3S)-2-chloro-3-methylvalerate (5M)

Compounds (1M)–(5M) were prepared by the same method. The synthesis of compound (1M) is described below.

4-(2-Propenyloxy)biphenyl-4′-ol (1) (2.5 g, 0.0112 mol) and (2S,3S)-2-chloro-3-methylvaleric acid(1.8 g, 0.0121 mol) dissolved in dry dichloromethane(150 mL), N,N-dicyclohexylcarbodiimide (DCC, 2.72 g, 0.0132 mol) and 4-(N, N-dimethyl-amino)-pyridine (DMAP, 0.1 g) were added to react under nitrogen. The reaction mixture was stirred for 24 h at room temperature. The solution was filtered and washed with an excess of dichloromethane. The filtrate was washed with water and dried over anhydrous magnesium sulfate. After removal of the solvent by evaporation under reduced pressure, the residue was purified by column chromatography on silica gel using hexane/ethyl acetate as eluent to yield 1.37 g (34%) of white crystals [mp = 97.3°C. ^{1}H-NMR (CDCl$_3$, δ, ppm): 0.90–1.06 (m, 3H, $-\mathrm{CH_2-C\underline{H}_3}$), 1.10–1.18 (m, 3H, $-\mathrm{CH-C\underline{H}_3}$), 1.30–1.55 (m, 2H, $-\mathrm{C\underline{H}_2-CH_3}$), 2.15–2.30 (m, 1H, $-\mathrm{C\underline{H}-CH_3}$), 4.38 (d, 1H, $-\mathrm{C\underline{H}Cl}$), 4.58 (m, 2H, $-\mathrm{O-C\underline{H}_2-CH{=}}$), 5.31 (m, 2H, $=\mathrm{C\underline{H}_2}$), 6.08 (m, 1H, $\mathrm{CH_2-C\underline{H}{=}}$), 6.90–7.58 (m, 8H, aromatic protons)].

Liquid Crystal Siloxane Compounds (1A)–(5A) and (1B)–(5B). Siloxane dimer synthesized from (1M) to (5M) are marked as (1A)–(5A) and siloxane trimer from (1M) to (5M) are marked as (1B)–(5B). Compounds (1A)–(5A) and (1B)–(5B) were prepared using the same method. The synthesis of compound (1B) is described below.

To a degassed solution of compound (1M) (0.29 g, 0.0008 mol) and heptamethyltrimethylsiloxyl (0.21 g, 0.0009 mol) in 15 mL of dry, freshly distilled toluene was added divinyltetramethyldimethylsiloxyl (2.5 mg) as catalyst. The reaction mixture was stirred at 70°C under nitrogen for 48 h. After the solvent being evaporated, the residue was purified by column chromatography (silica gel, using *n*-hexane/ethyl acetate as an eluent) to yield 0.30 g (64%) of white crystals [^{1}H-NMR (CDCl$_3$, δ, ppm): 0.0 (m, 21H, $-\mathrm{Si-C\underline{H}_3}$), 0.53 (m, 2H, $-\mathrm{Si-C\underline{H}_2-CH_2-}$), 1.10–2.40 (m, 11H, $-\mathrm{C\underline{H}_2-}$, $-\mathrm{C\underline{H}_2-C\underline{H}_3}$, and $-\mathrm{C\underline{H}-C\underline{H}_3}$), 4.01 (m, 2H, $-\mathrm{O-C\underline{H}_2-CH_2-}$), 4.38 (d, 1H, $-\mathrm{C\underline{H}Cl-}$), 6.90–7.58 (m, 8H, aromatic protons)].

Results and Discussion

In this study, we synthesized three series of compounds. Each series includes five different length spacers, such as 3, 6, 9, 10, and 11 methlene units. The first series of compound (1M)–(5M) represents a double bond in the end-tail position of the compounds; in the second series (1A)–(5A), a dimethylsiloxyl group is utilized to replace the double-bond tail end. For the third series (1B)–(5B), a trimethylsiloxyl group is substituted as the end-tail group. The molecular structure and the general synthetic procedures of these compounds are shown in Scheme 1, and all the final products are examined by the nuclear magnetic resonance spectrometer in order to verify the correction of the molecular structure.

The thermal and mesomorphic properties of compounds (1M)–(5M), (1A)–(5A), and (1B)–(5B) are measured using DSC and POM. The phase transition temperatures and enthalpy changes of compounds (1M)–(5M) with five different length spacers are listed in Table 1. Among them, the phase transition of compound (2M) displays an enantiotropic S_A phase, while compounds (3M) and (4M) show an enantiotropic S_A and a monotropic S_C* phase. Compound (5M) reveals both enantiotropic S_A and S_C* phases. The results demonstrate that the thermal stability of an S_C* phase increases as the spacer length increased.

The phase transition temperatures and enthalpy change of the compounds (1A)–(5A) and (1B)–(5B) are listed in Tables 2 and 3. The crystallization of compound (1A) is rather slow, and, therefore, the crystallization temperature cannot be observed during the DSC cooling scan down to −60°C. Compound (1B) is a transparent liquid under the room temperature, and no phase transition is detected by POM and DSC scanning between −60°C and 100°C. All the compounds (2A)–(5A) and (2B)–(5B) reveal both enantiotropic S_C* characteristic and S_A phases. Figure 1 depicts a DSC analysis diagram of compound (5A), and its liquid crystalline mesophases are observed by POM; Figure 2(a) shows the forcal-conic fan texture of S_A, while Figure 2(b) displays the broken focal-conic fan texture of S_C*.

In comparison of the thermal transitions of three series of compounds (1M)–(5M), (1A)–(5A), and (1B)–(5B), some conclusions are summarized as follows: (a) S_C* phase is formed when the carbon number of flexible spacer is larger than six for the vinyl precursors (1M)–(5M). (b) For both siloxane derivatives, (2A) and (2B) containing six methylene units in the spacer show enantiotropic S_C* phase. This means that incorporation of the

Table 1. Thermal transition of olefinic compounds (1M)–(5M)

Compound	*n*	Phase transitions, °C(corresponding enthalpy changes, Kcal/mole) $\frac{\text{heating}}{\text{cooling}}$
(1M)	3	$\frac{\mathrm{K}97.2(3.20)\mathrm{I}}{\mathrm{I}92.3(-3.16)\mathrm{K}}$
(2M)	6	$\frac{\mathrm{K}56.3(4.31)^{a}\mathrm{S_A}63.2(-)^{a}\mathrm{I}}{\mathrm{I}56.1(-)^{a}\mathrm{S_A}50.9(4.02)\mathrm{K}}$
(3M)	9	$\frac{\mathrm{K}38.5(5.94)\mathrm{S_A}43.7(1.0)\mathrm{I}}{\mathrm{I}50.5(-0.98)\mathrm{S_A}33.1(-0.08)\mathrm{S_C^*}17.6(-1.89)\mathrm{K}}$
(4M)	10	$\frac{\mathrm{K}46.0(4.98)\mathrm{S_A}52.9(0.85)\mathrm{I}}{\mathrm{I}48.8(-1.03)\mathrm{S_A}32.7(-0.06)\mathrm{S_C^*}22.4(-5.53)\mathrm{K}}$
(5M)	11	$\frac{\mathrm{K}49.5(5.03)\mathrm{S_C^*}55.0(-)^{b}\mathrm{S_A}56.4(0.83)\mathrm{I}}{\mathrm{I}53.2(-0.98)\mathrm{S_A}42.0(-)^{b}\mathrm{S_C^*}26.2(-5.52)\mathrm{K}}$

Note: K = crystal, S_A = smectic A, S_C* = chiral smectic C, I = isotropic.

[a] Overlapped transition.

[b] Determined by polarizing optical microscopic observation.

Table 2. Thermal transitions of dimethylsiloxyl-containing compounds (1A)–(5A)

Compound	*n*	Phase transitions, °C(corresponding enthalpy changes, Kcal/mole) $\frac{\text{heating}}{\text{cooling}}$
(1A)	3	$\frac{\mathrm{K}57.8(3.42)\mathrm{I}}{\mathrm{a}}$
(2A)	6	$\frac{\mathrm{K}14.7(0.71)\mathrm{S}_{\mathrm{C}}^{*}24.0(-)^{b}\mathrm{S}_{\mathrm{A}}41.9(0.21)\mathrm{I}}{\mathrm{I}32.8(-0.16)\mathrm{S}_{\mathrm{A}}20.1(-)^{b}\mathrm{S}_{\mathrm{C}}^{*}8.5(-0.69)\mathrm{K}}$
(3A)	9	$\frac{\mathrm{K}36.7(0.86)\mathrm{S}_{\mathrm{C}}^{*}48.2(0.06)\mathrm{S}_{\mathrm{A}}57.1(0.52)\mathrm{I}}{\mathrm{I}49.8(-0.23)\mathrm{S}_{\mathrm{A}}44.4(-0.02)\mathrm{S}_{\mathrm{C}}^{*}30.1(-0.92)\mathrm{K}}$
(4A)	10	$\frac{\mathrm{K}31.2(1.44)\mathrm{S}_{\mathrm{C}}^{*}47.0(0.04)\mathrm{S}_{\mathrm{A}}61.3(1.18)\mathrm{I}}{\mathrm{I}57.7(-1.02)\mathrm{S}_{\mathrm{A}}44.3(-0.04)\mathrm{S}_{\mathrm{C}}^{*}19.4(-0.79)\mathrm{K}}$
(5A)	11	$\frac{\mathrm{K}27.9(0.91)\mathrm{S}_{\mathrm{C}}^{*}52.8(0.05)\mathrm{S}_{\mathrm{A}}63.3(1.40)\mathrm{I}}{\mathrm{I}60.6(-1.18)\mathrm{S}_{\mathrm{A}}50.9(-0.03)\mathrm{S}_{\mathrm{C}}^{*}25.4(-0.89)\mathrm{K}}$

Note: K = crystal, S_A = smectic A, $S_C{}^*$ = chiral smectic C, I = isotropic.
[a] Enthalpy is very small.
[b] Determined by polarizing optical microscopic observation.

siloxane unit in an LC molecule has the tendency to stabilized the $S_C{}^*$ phase. (c) The LC compounds with tris-siloxane unit (2A)–(5A) show much lower melting points and wider $S_C{}^*$ temperature ranges than those LC compounds with bis-siloxane unit (2B)–(5B). Both compounds (4A) and (5B), which reveal an $S_C{}^*$ phase under the room temperature, can be used to formulate LC mixtures for display application.

According to the literature [20], side chain liquid crystal polysiloxane containing 4-hydroxyphenyl(2S,3S)-2-chloro-3-methylvalerate as mesogen owns higher transition temperature of nearly 40°C than small liquid crystal siloxane compound, although their temperature ranges of liquid crystal are close. Correspondingly, both the polymer with six carbon spacer length and the compound (2M) with six carbon spacer length have only S_A liquid crystalline mesophase; however, compounds (2A) and (2B) exhibit enantiotropic $S_C{}^*$ phases. This result shows that the small siloxane molecule is more helpful than the side chain polysiloxane for stabilizing the $S_C{}^*$ liquid crystalline mesophase. If it is assumed that longer spacer length is good for the formation and the stabilization of an $S_C{}^*$ phase in terms of the spacer concept for general liquid crystal mesophase, the molecules of dimethylsiloxyl and trimethylsiloxyl should be predicted to have the capability to increase the function of

Table 3. Thermal transitions of trimethylsiloxyl-containing compounds (1B)–(5B)

Compound	*n*	Phase transitions, °C(corresponding enthalpy changes, Kcal/mole) $\frac{\text{heating}}{\text{cooling}}$
(1B)	3	$\frac{(-)^{a}}{(-)^{a}}$
(2B)	6	$\frac{\mathrm{K}-2.2(0.34)\mathrm{S}_{\mathrm{C}}^{*}18.6(-)^{b}\mathrm{S}_{\mathrm{A}}36.0(0.41)\mathrm{I}}{\mathrm{I}25.6(-0.15)\mathrm{S}_{\mathrm{A}}10.8(-)\mathrm{S}_{\mathrm{C}}^{*}-10.0(-0.39)\mathrm{K}}$
(3B)	9	$\frac{\mathrm{K}35.2(0.48)\mathrm{S}_{\mathrm{C}}^{*}52.1(0.01)\mathrm{S}_{\mathrm{A}}61.4(0.05)\mathrm{I}}{\mathrm{I}52.4(-0.10)\mathrm{S}_{\mathrm{A}}44.9(-0.01)\mathrm{S}_{\mathrm{C}}^{*}28.8(-0.54)\mathrm{K}}$
(4B)	10	$\frac{\mathrm{K}29.5(0.86)\mathrm{S}_{\mathrm{C}}^{*}52.2(0.11)\mathrm{S}_{\mathrm{A}}59.8(0.91)\mathrm{I}}{\mathrm{I}55.8(-0.71)\mathrm{S}_{\mathrm{A}}49.5(-0.05)\mathrm{S}_{\mathrm{C}}^{*}26.6(-0.84)\mathrm{K}}$
(5B)	11	$\frac{\mathrm{K}20.4(0.75)\mathrm{S}_{\mathrm{C}}^{*}46.6(0.08)\mathrm{S}_{\mathrm{A}}56.4(0.71)\mathrm{I}}{\mathrm{I}53.5(-0.51)\mathrm{S}_{\mathrm{A}}45.0(-0.02)\mathrm{S}_{\mathrm{C}}^{*}16.7(-0.51)\mathrm{K}}$

Note: K = crystal, S_A = smectic A, $S_C{}^*$ = chiral smectic C, I = isotropic.
[a] Did not show any temperature transition when it was measured by DSC from −60°C to 100°C.
[b] Determined by polarizing optical microscopic observation.

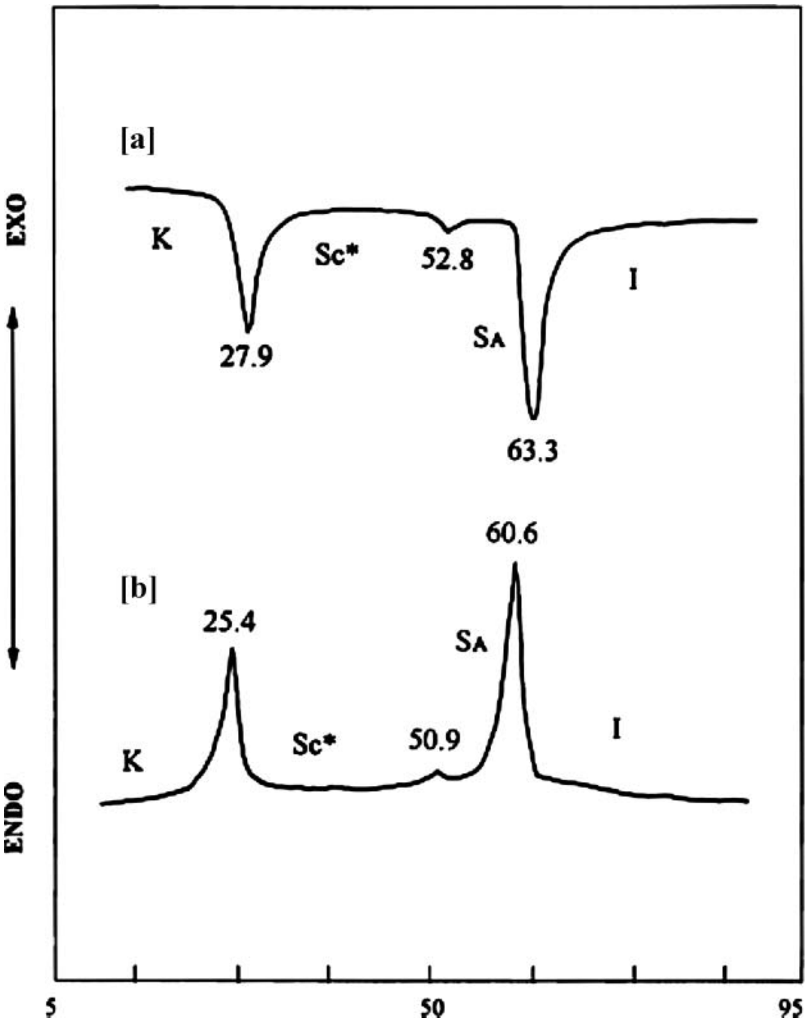

Figure 1. DSC thermograms of compound (5A) (10°C/min) for (a) second heating scanning and (b) cooling scanning.

effective spacer length. Besides, in contrast of the $S_C{}^*$ transition property between compounds (2A) and (5M), dimethylsiloxyl group shows the equal effect as five-carbon length spacer in the thermoproperty. The rest may be inferred by the analogy, compound (5A) with the effective spacer length counted as 16 units of carbon chain, and this long carbon chain certainly produced no side chain crystallization phenomenon. This situation demonstrates two advantages: the first is that the small siloxane molecule has the increasing function of effective spacer length; the second is that siloxane molecule will not result in the side chain crystallization. Therefore, it is suitable for applying to the synthesis of smectic liquid crystal compound.

Compounds (3M)–(5M), (3A)–(5A), and (3B)–(5B) were filled into a 4-mg thick cell, made of indium tin oxide glass, whose surface was coated by polyimide which was rubbed in parallel direction. Voltage (about 5 V/μm) of 50 Hz frequency and 20 Vp (peak

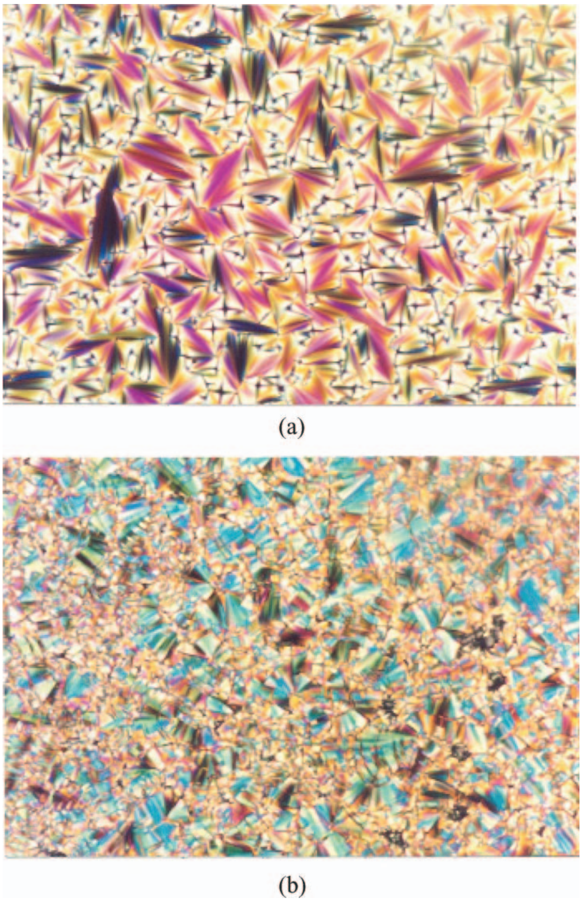

Figure 2. Polarizing optical micrographs (magnification ×320) of compound (5A) in (a) S_A texture obtained from isotropic phase after cooling to 55°C and (b) S_C^* texture obtained after cooling to 40°C.

voltage) was used, and the measurement area was 0.26 cm^2. The sample was heated to an isotropic temperature, adding voltage to sample at cooling process. Measurements of *Ps* value and rotational viscosity were taken every 0.5–1°C during the S_C^* mesophase range. Due to the lack of cooling accessory, the lowest temperature of measurement was the room temperature.

The *Ps* value and rotational viscosity of various compounds have the tendency to fall down when the temperatures increase. In Figure 3, the *Ps* value quickly becomes larger to 255 nC/cm^2 and rotational viscosity also becomes higher when the temperature of compound (5A) falls down from 26°C to 25.7°C. Similarly, the *Ps* value becomes higher when the temperature of compound (4B) falls down from 28°C to 27.6°C. This result exhibits that there is a higher *Ps* value when the temperatures of compounds (5A) and (4B) fall down from an S_C^* phase to a neighboring crystallization temperature.

In summary, this study indicates that the synthesized FLCs with siloxane have not only the wider S_C^* phase, but also a larger spontaneous polarization. These compounds have great potential to be applied to the ferroelectric liquid crystalline display monitor.

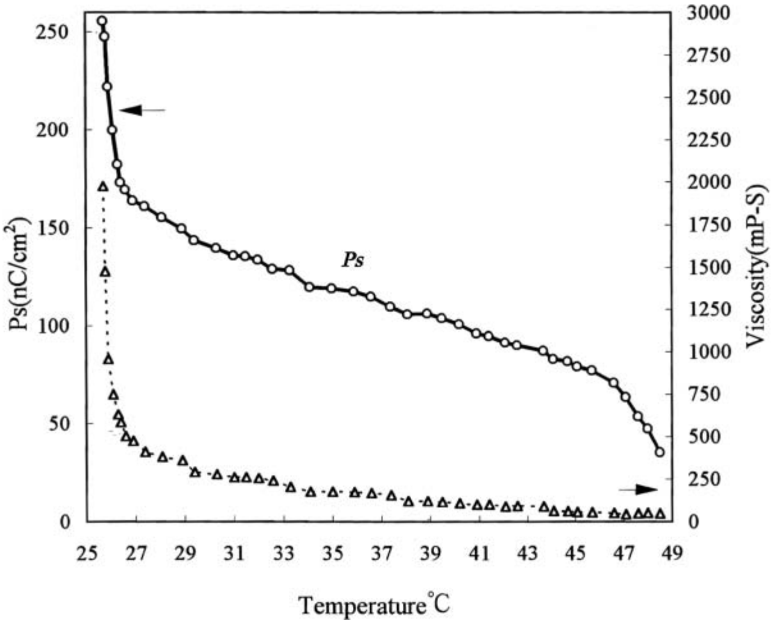

Figure 3. Spontaneous polarization (*Ps*) and viscosity vs. temperature for compound (5A).

Conclusions

The siloxane molecule induction is helpful to the S_C* formation and S_C* stabilization, and simultaneously it causes the liquid crystal temperature range of S_C* to be broader. Carbon chain length higher or equal to 6 units of compounds (2A)–(5A) and (2B)–(5B) will possess an enantiotropic S_C* phase. The siloxane molecule has the ability to increase "effective spacer length," and it is also assistance in the formation of S_C* phase and the stabilization of S_C* liquid crystalline mesophase. Furthermore, the siloxane molecule will not induce side chain crystallization phenomenon and dilute *Ps* value. Therefore, the siloxane molecule can lower the mesophase transition temperature of the liquid crystal compound, and simultaneously it can widen the temperature range of S_C* liquid crystalline mesophase, especially the trimethylsiloxyl group.

References

[1] Mayer, R. B., Liebert, L., Strzeleckl, L., and Keller, P. (1975). *J. Phys. Lett.*, *36*, 69.
[2] Goodby, J. W. (1991). *Ferroelectric Liquid Crystals: Priperties and Applications*, Gordon and Breach Science Publishers: New York.
[3] Mcardle, C. B. (1989). *Side Chain Liquid Crystal Polymers*, Chapman and Hall Publishers: New York.
[4] Deb, R., Nath, R. K., Paul, M. K., Rao, N. V. S., Tuluri, F., Shen, Y., Shao, R., Chen, D., Zhu, C., Smalyukh, I. I., and Clark, N. A. (2010). *J. Mater. Chem.*, *20*, 7332.
[5] Perkins, S. P., Shoosmith, D. E., and Coles, H. J. (2001). *Mol. Cryst. Liq. Cryst.*, *364*, 943.
[6] Scherowsky, G., Schliwa, A., Springer, J., Kuhnpast, K., and Trapp, W. (1989). *Liq. Cryst.*, *5*, 1281.
[7] Shibaev, V. P., Kozlovsky, M. V., and Plate, N. A. (1990). *Liq. Cryst.*, *8*, 1281.

[8] Vallerien, S. U., Kremer, F., and Fischer, E. W. (1990). *Makromol. Chem. Rapid Commun.*, *11*, 593.

[9] Kapitza, H. and Zentel, R. (1991). *Makromol. Chem.*, *192*, 1859.

[10] Endo, H., Hachiya, S., Uchida, S., Hashimoto, K., and Kawasaki, K. (1991). *Liq. Cryst.*, *9*, 635.

[11] Vallerien, S. U., Kremer, F., Kapitza, H., Zentel, R., and Fischer, E. W. (1990). *Ferroelectrics*, *109*, 273.

[12] Lagerwall, S. T. and Dahl, I. (1984). *Mol. Cryst. Liq. Cryst.*, *114*, 151.

[13] Lagerwall, S. T., Otterholm, B., and Skarp, K. (1987). *Mol. Cryst. Liq. Cryst.*, *152*, 503.

[14] Roberts, J. C., Kapernaum, N., Giesselmann, F., Wand, M. D. and Lemieux, R. P. (2008). *J. Mater. Chem.*, *18*, 5301.

[15] Grüneberg, K., Naciri, J., and Shashidhar, R. (1996). *Chem. Mater.*, *8*, 2486.

[16] Keith, C., Reddy, R. A., Baumeister, U., and Tschierske, C. (2004). *J. Am. Chem. Soc.*, *126*, 14312.

[17] Naciri, J., Ruth, J., Grawford, G., Shashidhar, R., and Ratna, B. R. (1995). *Chem. Mater.*, *7*, 1397.

[18] Hsu, C. S. and Her, B. S. (1996). *Macromol. Chem. Phys.*, *197*, 4105.

[19] Liao, C. T., Wu, Z. L., Wu, N. C., Liu, J. Y., Jiang, M. H., Zou, S. F., and Lee, J. Y. (2010). *Mol. Cryst. Liq. Cryst.*, *533*, 3.

[20] Hsu, C. S., Liu, M. C., and Lu, Y. H. (1994). *J. Polym. Res.*, *1*, 321.